Empirically modeling ionospheric electron density variations using *F107*, *E107* and *MgII* indices based on long-term incoherent scatter radar observations over Millstone Hill

Shun-Rong Zhang and John M. Holt

MIT Haystack Observatory,
Route 40, Westford, MA 01886, USA

Abstract.

Each of three solar flux indices, *F107*, *E107*, and *MgII* core-to-wing, has been tested as a solar activity proxy to model empirically electron density *Ne* measurements made by an incoherent scatter radar during the period of 1976-2001 over the height span of 150-1000km at Millstone Hill. It is found that deviations of model values given by the three indices to the data are practically the same, regardless of altitude, local time, and season, indicating no significant improvements with introducing the newer indices *E107* and *MgII* for empirically modeling long-term *Ne* data. The long-term behavior of the three indices are identical. This paper also discusses electron density responses to the solar flux index.

1.0 Introduction

Since the 1960s, incoherent scatter (IS) measurements of electron density Ne, electron temperature Te, ion temperature Ti, and line-of-sight ion drifts have been acquired over Millstone Hill. A robust WWW-based database system, called Madrigal, contains about one thousand experiments offered by the zenith antenna observations since 1976 and the steerable elevation-scan antenna observations since 1980. The large volume of data makes it possible to better understand ionosphere-thermosphere features qualitatively and quantitatively for sub-auroral regions in the Northern America, and to serve space weather needs as well.

One way to represent the data is to construct empirical models [Holt et al., 2002]. A variety of variations in the ionosphere, including temporal and spatial, and solar activity and geom.agnetic activity dependences, have to be considered and determined. At mid-latitudes, ions are primarily created by photoionization due to the solar EUV flux. Thus the level of solar variation is an important component of any ionospheric model, and appropriate solar flux indices are essential for the success of such models. The sun-spot number *R* and 10.7 cm flux index *F107* are well-known traditional indices for atmospheric modeling. Newer solar irradiation indices, such as *MgII* core-to-wing ratio [Viereck and Puga, 1999] and *E107* [Tobiska et al., 2000], are being proposed as better proxy to represent the solar

EUV flux entering the thermosphere. This paper reports our modeling results of ionospheric electron density over 150 -1000 km using 3 solar flux indices, *F107, E107,* and *MgII*. We first describe our data processing and modeling method, "bin-fit" technique, then concentrate on electron density responses to solar flux changes, and the goodness-of-fit for the modeling to represent the model-data difference for each of indices. We summarize our conclusions in the last section.

2.0 Bin-fit technique

The bin-fit technique combines data binning with least squares fitting. The measured *Ne* data is sorted into bins according to local time, altitude, and the day of year (to represent seasonal variations). The bin size is 1 hour for local time and 61 days for the seasonal variation. 14 altitude bins centered at 150, 175, 200, 225, 250, 300, 350, 400, 450, 500, 550, 600, 800, and 1000 km, are employed for data within 39-45^{o}geodetic latitude.

In each bin, a sequential least-square fit based on Givens transforms [Gentleman, 1973] is performed to determine the dependencies on solar and magnetic activity using the following equation:

$$Ne = \beta 0 + (\beta 1 \times f) + (\beta 2 \times a) + (\beta 3 \times f \times a)$$

where βs are fitting coefficients, and $a = (ap - 15)/15$ is the normalized Ap index. f is the normalized solar flux index. When *F107* is chosen, $f = (F107 - 135)/135$, where *F107* is the previous day's solar 10.7 cm flux; when *E107* is chosen, $f = (E107 - 135)/135$, where the daily *E107* value is used; when *MgII* is chosen, $f = (MgII \times 1000 - 135)/135$, where we multiply the daily *MgII* index by 1000 to give an appropriate order of magnitude similar to *F107* and *E107*. The *E107* data is created by the SOLAR2000 model [Tobiska et al., 2000], and the *MgII* data is from the NOAA Mg II daily Index version 9.1 [Viereck, et al., 2001].

3.0 Linear relationship between *Ne* and solar flux index

Electron density increases with increasing solar flux due to enhanced photoionization. The linear increase is generally true, and prevails particularly under low to middle levels of solar activity. The increase is found to be "saturated" for very high solar *F107* index, because the EUV flux exhibits a similar nonlinear pattern of increase and saturation [Balan et al., 1994]. Our data further suggests the importance of atmospheric composition [Richards, 2001] and dynamics effects, since the saturation evolves with altitude and local time during the day and from winter to summer. It is present under conditions when O/N2 effects [Rishbeth and Setty, 1961] has a significant influence on the F2 layer O+ density, such as near the F2 peak altitude and during winter. Figure 1 shows the binned *Ne* data for the November-December period at center altitude of 250 km for 1400 LT, plotted against *F107* (panel a), *E107* (panel b), and *MgII* (panel c). It is seen that the nonlinear effects of electron density response still exist for the *E107* and *MgII* indices.

This density saturation is accompanied by a similar slow increase in the ion temperature measurement for very high solar activity (Figure 2). Since the ion temperature for low ionospheric altitudes is a reasonable measure of the neutral temperature, it can be expected, in response to much intensified solar activity, that the neutral composition effects should indeed come into play for the *Ne* saturation.

4.0 Comparisons of χ^2 values

Different effects of the three solar flux indices on modeling *Ne* variations can be seen by examining the model-data difference, or goodness-of-fit, which is defined by $\chi^2 = (Model - Data)^2/N$, the mean squared deviation where N is the number of data within the bin. Shown in Figure 3 are diurnal variations of $\log(\chi^2)$ obtained with each solar index for typical altitude and month. The goodness-of-fit is small when *Ne* is small: the deviation is smaller in summer than in winter, following the *Ne* seasonal variation caused by the changes of O/N2 ratio [Rishbeth and Setty, 1961]; it is smaller below and above the F2 peak range; it is generally larger during the day.

It is seen that *F107* and *E107* indices lead to actually the identical goodness-of-fit, regardless of altitude, season, and local time. The F10.7 index represents the solar coronal emissions; the *E107* is the solar EUV flux at the top of the Earth's atmosphere integrated over chromospheric and coronal emissions. However, as pointed out by Tobiska [2001], the long-term *E107* and *F107* behavior is nearly identical, so both indices should give very similar results in representing the long-term ionospheric variations.

MgII results are basically close to and never exceed the goodness-of-fit level set by the *F107* and *E107* indices. In particular, for summer around the F2 peak region, the *MgII* index tends to yield a slightly smaller model-data difference. We note that the *MgII* data that we have obtained starts in November 1978, while our *Ne* data is available since February 1976. Thus in our analysis we are forced to drop all our *Ne* data during the *MgII* data gap. This gap results in about 5% loss of data points. To check if the difference in data amount has contributed to the slight disagreement of results for the three indices, we performed the modeling with *F107* and *E107* indices using the same data as for *MgII* modeling (i.e., removing the data before November 1978), and we found excellent agreement in the goodness-of-fit given by the three.

5.0 Conclusion

Long-term incoherent scatter radar measurements of electron density over Millstone Hill have been fit by an empirical model dependent upon a solar flux index. We have tested three solar flux indices, the traditional *F107*, and the newer *E107* and *MgII* core-to-wing, to determine which index yields a better fit to the data. The latter two indices are considered to better represent the solar EUV flux entering the Earth's atmosphere. We found that deviations of model values given by the three indices to data are practically the same,

regardless of altitude, local time, and season, indicating no significant improvements from introducing the newer *E107* and *MgII* indices for empirically modeling long-term *Ne* data. The long-term behavior of the three indices are identical.

We also find that electron density responses to the increasing solar activity are to linearly increase for low and moderate solar activity, but the increase tends to be saturated for very high solar activity. This latter phenomenon is accompanied by a similar "saturation" in the ion temperature measurements, indicating possible atmospheric composition contributions.

Acknowledgements.

We thank the members of the Haystack Observatory Atmospheric Sciences Group for assembling and maintaining the Madrigal Database of Millstone Hill incoherent scatter radar observations, which were the basis of this study. This research was supported by NSF Space Weather Grant ATM-9819413. The Millstone Hill incoherent scatter radar is supported by a cooperative agreement between the National Science Foundation and the Massachusetts Institute of Technology. We thank W. Kent Tobiska for supplying the SOLAR2000 model. The *MgII* c/w data has been obtained through the WWW site http://sec.noaa.gov/ftpmenu/sbuv.html.

Reference.

Balan, N., G. J. Bailey, B. Jenkins, P. B. Rao, and R. J. Moffett, Variations of ionospheric ionization and related solar fluxes during an intense solar cycle, *J. Geophys. Res.*, 2243-2253, 1994.

Gentleman, W. V., Least squares computations by Givens transformations without square roots, *J. Inst. Math. Applics.*, 12, 325-336, 1973.

Holt, J. M., S.-R. Zhang, and M. J. Buonsanto, Regional and local ionospheric models based on Millstone Hill incoherent scatter radar data, *Geophys. Res. Letts*., 29, 10, 1029/2002GRL014678, 2002

Richards, P. G., Seasonal and solar cycle variations of the ionospheric peak electron density: Comparison of measurement and models, *J. Geophys. Res.,* 106, 12,803-12,819, 2001.

Rishbeth, H., and C. S. G. K. Setty, The F-layer at sunrise, *J. Atmos. Terr. Phys*., 20, 263-276, 1961.

Tobiska, W. K., Validating the solar EUV Proxy, E10.7, *J. Geophys. Res.,* 106, 29,969-29,978, 2001.

Tobiska, W. K., T. Woods, F.,Eparvier, R. Viereck, L. Floyd, D. Bouwer, G. Rottman, and O. R. White, The SOLAR2000 empirical solar irradiance model and forecast tool, *J. Atmos. Terr. Phys*., 62, 1233-1250, 2000.

Viereck, R., and L. Puga, The NOAA Mg II core-to-wing solar index: Construction of a 20 year timeseries of chromospheric variability from multiple satellites, *J. Geophys. Res.,* 104, 9995-10005, 1999.

Viereck, R., L. Puga, D. McMullin, D. Judge, M. Weber, W. K. Tobiska, The Mg II index: A proxy for solar EUV, *Geophys. Res. Letts*., 28, 1343-1346, 2001.

Figure 1.

Figure 1. Saturation of electron density responses to solar flux represented by (a) *F107* index, (b) *E107* index, and (c) *MgII* core-to-wing index. The green dots are for quieter geomagnetic conditions with Ap index smaller than its average for the entire data of this bin. The rest part of data is represented by red dots.

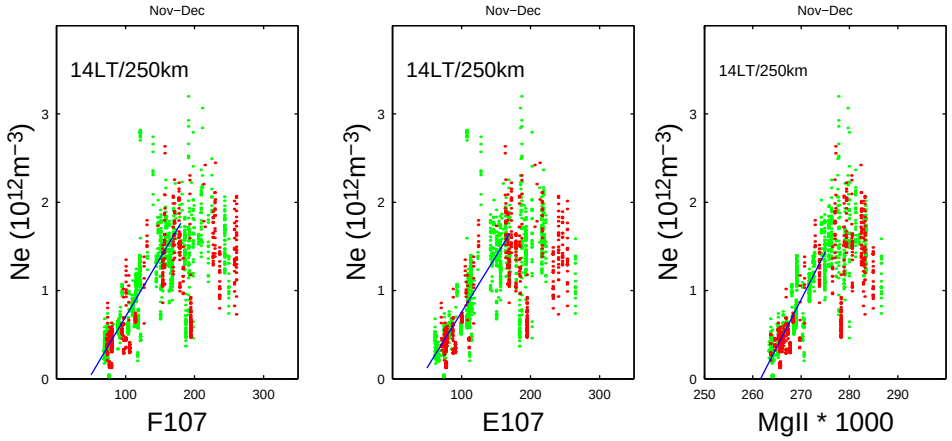

Figure 2.

Figure 2. Ion temperature responses at 225 km to solar *F107* index. The green dots are for quieter geomagnetic conditions with Ap index smaller than its average for the entire data of this bin. The rest part of data is represented by red dots.

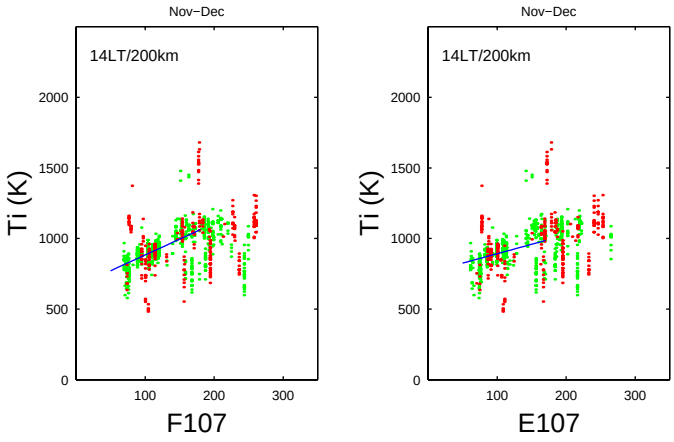

Figure 3.

Figure 3. Diurnal variations of the goodness of fit for 6 seasonal and 5 altitude bins